ICANS-XIII
13th Meeting of the International Collaboration on
Advanced Neutron Sources
October 11-14, 1995
Paul Scherrer Institut, 5232 Villigen PSI, Switzerland

ON THE PRESSURE WAVE PROBLEM IN LIQUID METAL TARGETS FOR PULSED SPALLATION NEUTRON SOURCES

Karel Skala, Günter S. Bauer

Paul Scherrer Institut, 5232 Villigen PSI, Switzerland

ABSTRACT

A liquid metal target for a pulsed spallation neutron source was modelled on the computer to investigate the effect of the high instantaneous power deposition (60 kJ in 1 μs) on the pressure in the liquid and the resulting stress on the container. It was found that for the short pulse duration the resulting stress would be likely to exceed the allowable design stress for steels of the HT-9 type with low nickel content. Adding a small volume fraction of gas bubbles might be a way to suppress almost completely the generation of pressure waves.

1. Introduction

Using a molten heavy metal as target material for spallation neutron sources has so far been considered mainly for continuous sources like ING [1] and SINQ [2]. The obvious advantages are

- a high heat removal capacity by the moving target material
- the absence of cooling water and its related problems of radiolysis and corrosion in the target region
- no structural radiation damage in the target material
- high heavy metal density in the interaction region (no dilution by cooling channels)
- volatile or potentially volatile spallation products can be removed "on line"
- a low specific afterheat due to a large target mass, which, together with the fact that the liquid can be drained into a dump tank, makes forced cooling during exchange operations not necessary.

In view of these attractive features and of the risk of damage in solid targts in pulsed spallation sources of high power level like the 5 MW for the European Spallation Source

Keywords: Liquid target, Pressure waves, Mercury, Stress

Project (ESS) [4], the question was investigated whether a liquid target could be used also in this case. One of the main differences between a pulsed and a continuous spallation neutron source is the very high instantaneous power (100 kJ per pulse for ESS) injected into the material during very short times at high repetition rate, (1 μs at 50 Hz). About 60% of the beam energy are deposited in the target which under these conditions, cannot be accommodated by thermal expansion during the pulse and will give rise to pressure waves that can result in substantial stress loads on the container wall. Although the material for the container wall can - within limits - be chosen for high mechanical stability, it is of prime importance to keep the load in a safe regime for long time operation even under the effect of radiation damage. In the present paper we report on preliminary calculations to examine these problems.

2. The physics model

Under the assumption that the target material will be either Pb, Pb-Bi eutectic or Hg in the liquid state we exclude the effect of phase transitions and related latent heat effects. All deposited energy will therefore be converted into heat, leading to thermal expansion. In view of the short duration of the energy pulse, this expansion is strongly hindered by the surrounding material and a force will be excerted that causes a pressure wave to travel through the material. Since this means acceleration and motion of material, it will have an immediate feedback effect on the pressure which must be taken into account through a coupling loop. Fig. 1 shows the conceptual basis of the calculations:

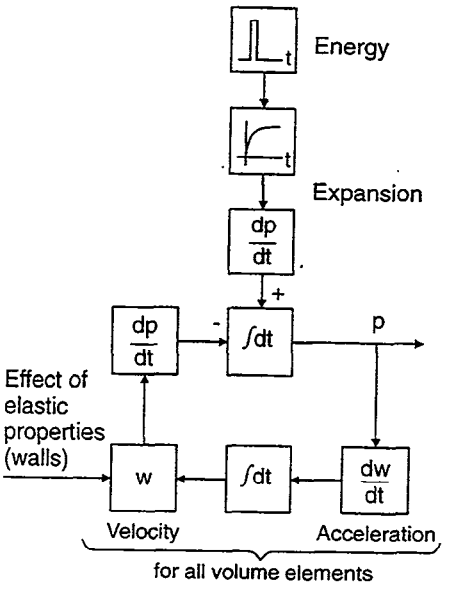

Figure 1: Simplified scheme of the calculational procedure to examine pressure waves in a liquid metal target. Accelerations and displacements are only allowed to occur to the extent permitted by the elastic properties of the system. Otherwiese they are treated as "virtual" and used to calculate the change in local pressure.

The pulse-like deposition of a large amount of energy in any volume element of the target is short enough, so that no change in volume is possible (isochoric case). It gives rise to a subsequent (hindered) expansion of the material whose time constant can be varied. The result is an increase of pressure as a function of time. This pressure is the cause of acceleration of the surrounding material, whose velocity is again obtained via an integration over time. The motion of this material will reduce the local pressure, giving rise to feedback

between the volume elemtens in the target. The pressure wave will thus travel through the material, mediated by the finite compressibility. It will pass through the non-heated zones of the target and reach the wall where it causes mechanical stress. Due to the elastic properties of the wall it will be reflected back into the material, giving rise to superposition. In a solid this might occasionally result in negative pressures (tensile stress) in the material. In the liquid we assume voiding to occour and hence we limit the minimum pressure to a small negative value or to zero (optional). At present we do not account for the latent heat of vaporization required to fill the void with metal vapour, nor do we account for any short term underswing of the pressure due to cohesive forces in the liquid, delaying the void formation. Both effects could be incorporated into the model for at a later stage if considered important and if sufficient information is available. Neglecting them keeps us on the safe side in terms of stress on the walls.

3. The geometrical model

The geometrical model is three dimensional but at present only elliptical target cross sections have been implemented (including, of course, the circular cross section as a special case). The target is taken long enough for its downstream end (parallel to the proton beam) not to affect the pressure during the time intervals considered (a few hundred μs). For the upstream end (beam entry point) one of three options can be selected

- an open surface
- a rigid flat cover
- an elastically flexible domed cover

In the case of an open surface, target material is allowed to leave the surface under the effect of the following forces

- pressure inside the liquid
- gravity
- inertia
- internal friction caused by viscosity.

The liquid volume, as well as the surrounding walls are subdivided into triply indexed elements limited by surfaces in the following way (Fig. 2).

- planes perpendicular to the beam axis (index I)
- cylinders concentric to the beam axis (index K)
- planes containing the beam axis (index L)

The volume elements can be defined as belonging to the liquid or as representing solid material. In the latter case tensile forces and shear stress are allowed to occur.

4. The mathematical model

All dynamical processes are described by algebraic relations and differential equations. The latter ones are solved by numerical integration. The pressure resulting in a medium is given by the general relation

$$dp = \left(\frac{\partial p}{\partial V}\right)_T dV + \left(\frac{\partial p}{\partial T}\right)_V dT \qquad (1)$$

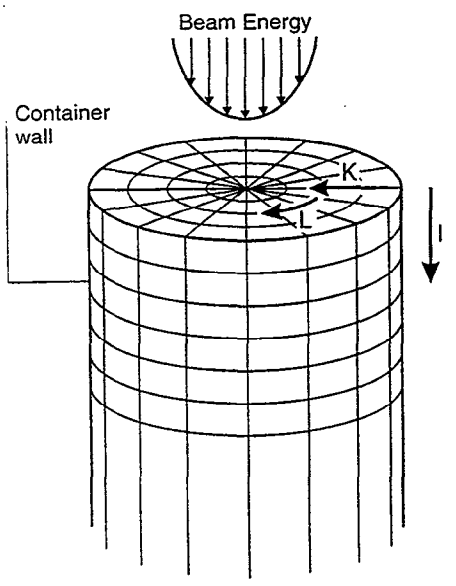

Figure 2: Scheme for the subdivision of the target volume into elements by surfaces and assignment of the indices I, K, L.

During the very short energy pulses no volume change can occur and hence only the second term in equation (1) is important (isochoric case). Following the energy deposition the resulting pressure will spread adiabatically in the medium and the first term in eqn. (1) becomes dominant because in liquid and solid media the adiabatic compression occurs practically without any change in energy, since c_p and c_v, the specific heat capacities at constant pressure and at constant volume are almost equal. The temperature rise caused by depositing an amount of energy E_d in a volume of mass m is then given by

$$\Delta T = \frac{E_d}{m \cdot c_v} \tag{2}$$

In our practical calculations the small change in temperature during the adiabatic expansion is in fact taken into account as shown in the appendix A1. where a derivation of the formulae used is given.

The result is a pressure increase Δp given by

$$\Delta p = \frac{c_p}{c_v} \cdot K \cdot \frac{\Delta V}{V_0} = \tilde{K} \cdot \frac{\Delta V}{V_0} \tag{3}$$

where K is the isothermal modulus of volume elasticity,

$$K = V_0 \left(\frac{\partial p}{\partial V} \right)_T \tag{3a}$$

and $\tilde{K}$ shall be called the "adiabatic modulus of volume elasticity". Using this quantity accounts for the change in temperature during adiabatic expansion. This allows us to drop the condition of short pulses and use our system of equations also for longer pulses (e.g. a 500 μs pulse of a long pulse souce).

The force excerted on any given volume element is the result of three components

- the difference in pressure on both sides
- friction caused by viscosity
- gravity.

The net force on any volume elemtent causes acceleration of the material which, through integration over time, finally yields a theoretical net displacement of the material. For each volume element the velocities and net displacements are calculated for the six faces of the element (Fig. 3). This allows to calculate a ficticious ("virtual") change in volume

$$\Delta V = \sum_{i=1}^{6} S_i \cdot B_i \tag{4}$$

with S being the area of the surface under consideration and B the displacement. We call the volume change "virtual" because it does not occur in reality but is the cause of a change in pressure as shown in Fig. 1.

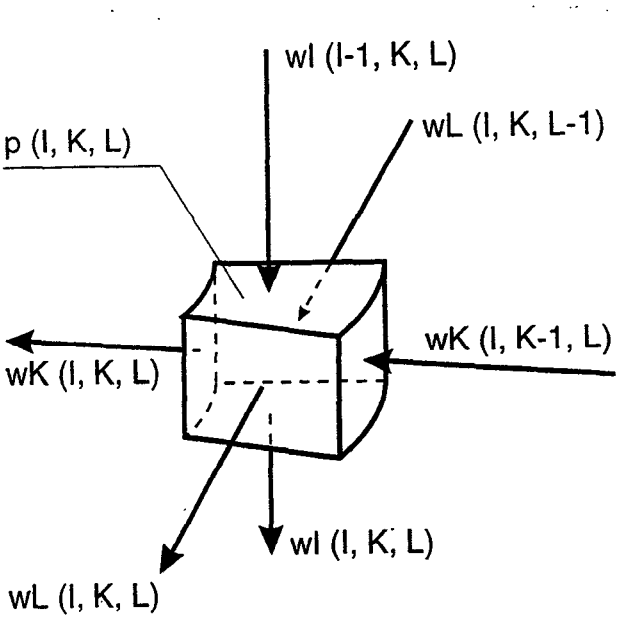

Figure 3: Velocities and displacements contributing to the "virtual" change in volume of a target element.

In this way the spreading of the pressure is followed through the target material as a function of time until it reaches the container wall. Due to the tensile strength of the wall, the pressure gives rise to stress in the wall material which is the sum of the direct pressure load on the surface element under consideration and the influence of the neighbouring elements, where the pressure wave may arrive at a different time. The toal stress is therefore a combination of pure tensile and stress (Fig. 4). The bending stress is calculated in analogy to the case of a beam with two fixed ends under lateral displacement.

The options mentioned for the beam entry face are treated in the following way:

- for the free surface the pressure above the liquid is set to zero and the equations of motion are used without restrictions

- for the rigid flat cover no displacements, velocities or accelerations are allowed at the boundary surface, i.e. the boundary surface acts as a "mirror".

- the domed flexible cover is treated in analogy to the elastic cylinder wall accounting for the double curvature in this case.

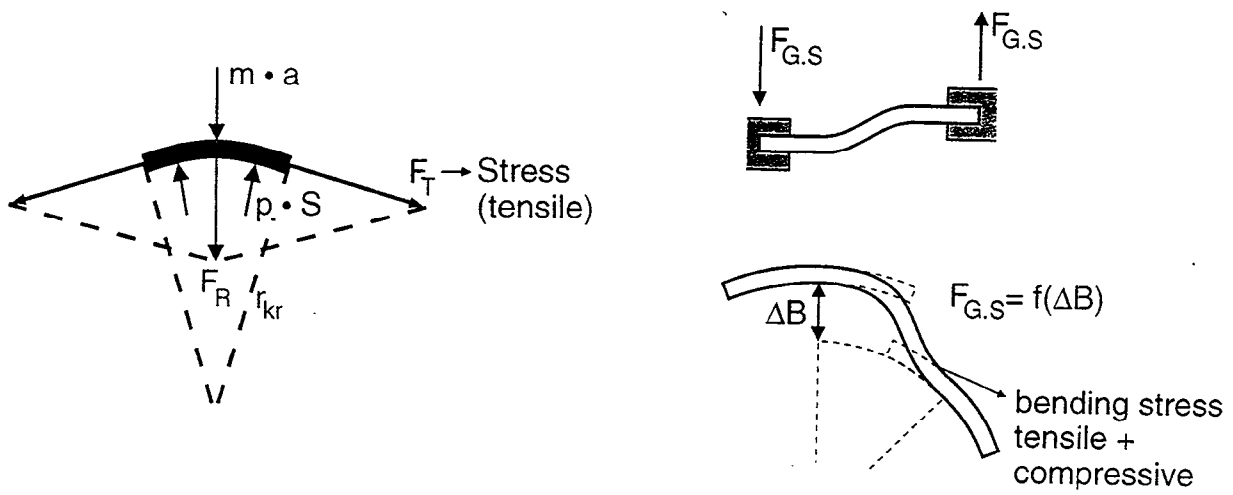

Figure 4: Modelling of different stress contributions in the target container wall.

5. The effect of the elastic modulus of the liquid

According to eqn. (3) the pressure rise in the liquid is directly proportional to its elastic modulus K_c, resp. $\tilde{K}_c$. Accounting for the fact that gases are orders of magnitude more compressible than solids or liquids, we assume that a small amount of gas bubbles can be continuously added to the region where the interaction between the target material and the proton beam takes place.

Any change in volume of the mixture ΔV_m will then be the sum of the change in volume of the gas ΔV_g and of the liquid ΔV_l:

$$\Delta V_m = \Delta V_g + \Delta V_l \tag{5}$$

According to eqn. (3) the second term is given by

$$\Delta V_l = -\frac{V_{l,0}}{K} \cdot \Delta p \tag{6}$$

In order to determine the first term of eqn. (5), we need to know whether the compression is isothermal or adiabatic. This depends on the rate of heat exchange between the metal and the gas, which should be high due to the smallness of the bubbles and their large surface. On the other hand the compression is very fast which would favour the adiabatic case. The general case is a polytropic compression

$$p \cdot V_g^n = p_0 \cdot V_{g,0}^n \quad with \quad 1 \le n \le \kappa \tag{7}$$

where n=1 holds for the isothermal and n = κ holds for the adiabatic case.

Calling the volume fraction of gas bubbles ε with

$$\varepsilon = \frac{V_{g,0}}{\left(V_g + V_l\right)_0} \tag{8}$$

it is easy to show (see appendix A2) that the modulus of elasticity for the mixture is given by

$$K_m = \left\{ \frac{1}{K_l} + \frac{1}{n} \cdot p_0^{\frac{1}{n}} \cdot \varepsilon \cdot p^{-\frac{n+1}{n}} \right\}^{-1} \tag{9}$$

For the case of mercury ($K_l = 2.77 \cdot 10^{10}\ \frac{N}{m^2}$) this quantity is shown in Fig. 5a and b as a function of pressure for various values of ε and for n=1 and n=1.63 (isothermal and adiabatic compression respectively). It is obvious that in the adiabatic case K and, as a consequence of the feedback also p, are much smaller than in the isothermal case, but the effect at moderate pressure levels is enormous even for very small values of ε, of the order of a few percent. We can therefore anticipate that, due to the high compressibility of the gas bubbles, there will be almost no overall pressure increase in the liquid as long as the total volume of the gas bubbles is sufficient to absorb the total volume increase in the liquid at moderate pressure increase in the gas.

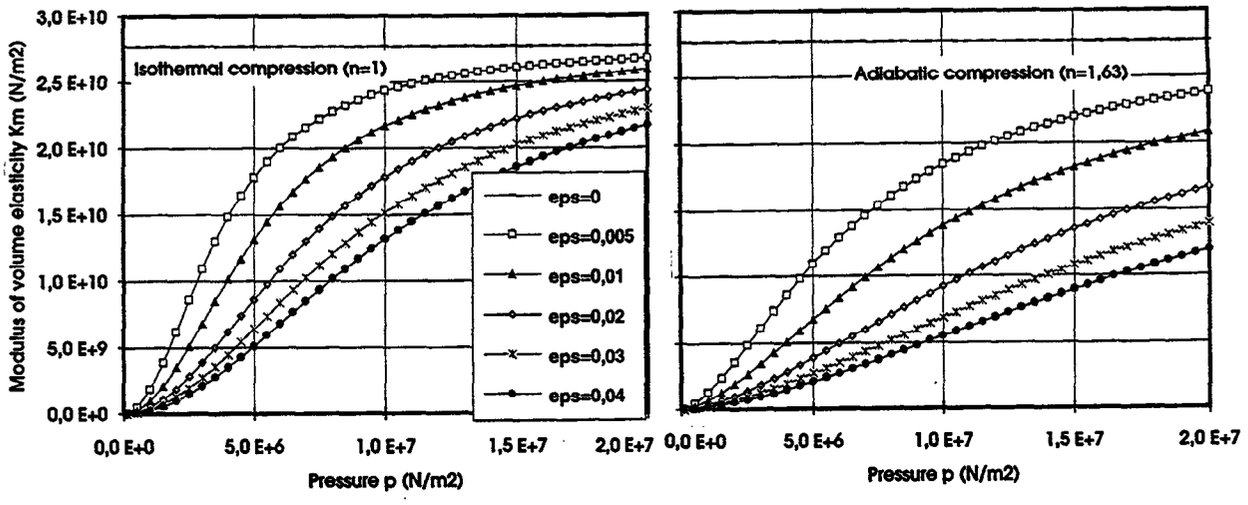

Figure 5: Dependence of the modulus of volume compressibility K_m of a mixtrue of liquid and gas on the pressure for different volume fractions of gas, ε. (a) iothermal case (b) adiabatic case.

For very small volume fractions of ε, on the other hand there may exist a positive feedback in pressure development because, while energy is initially stored in the compression of the bubbles, K_m increases rapidly towards the value of K_l and the pressure wave will spread as in the bubble-free case. However, as soon as the pressure starts dropping the energy stored in the bubbles will be released, causing the pressure to drop more slowly and eventually to give rise to interference maxima which may exceed the values obtained in the bubble-free case. Of course, these effects are strongly geometry dependent, too, and detailed calculations are needed for each sitation. As a general rule it may be stated however that, if gas bubbles are used to suppress the pressure waves, a volume concentration slightly above the "critical" one is much safer than one below. More details are given in the following chapter.

6. Some examples of results obtained so far

Our main interest in the current context are the stress levels induced in the container walls as a function of the various parameters and the target geometry. For the time being, the following effects are completely neglected

- static or quasi-static stress caused by temperature gradients in the walls
- static stress caused by hydraulic pressure
- stress caused by flow reversal at the beam entry window
- etc.

For the energy deposition in the liquid we assumed that about 60% of the beam energy are deposited in the target material, i.e. 3 MW time average or P_p = 60 kJ per pulse for the ESS case. The spatial distribution is taken as essentially exponential along the beam axis and as parabolic in radial direction with a base width of $2r_s$=10 cm. For each volume element the heating during the pulse is then given by

$$P(r,z) = c_{it} \cdot V_e \left(1 - \exp\left(-\frac{z - z_a}{\lambda_a}\right)\right) \cdot \left(\exp(-\Sigma \cdot z)\right) \cdot \left(1 - \left(\frac{r}{r_s}\right)^2\right) \qquad (10)$$

where V_e is the volume of the element under consideration, λ_a is a buildup length taken as 6.5 cm, z_a is an extrapolation length (1.77 cm), Σ is the macroscopic cross section of mercury for 1.3 GeV protons (0.07 cm^{-1}) and c_{it} is a quantity determined by iteration under the condition that the sum over all volume elements must give the value P_p. The numbers chosen are based on a compilation generated for the German SNQ project [3]. Fig. 6 shows the axial dependence of the power deposition integrated over the beam diameter.

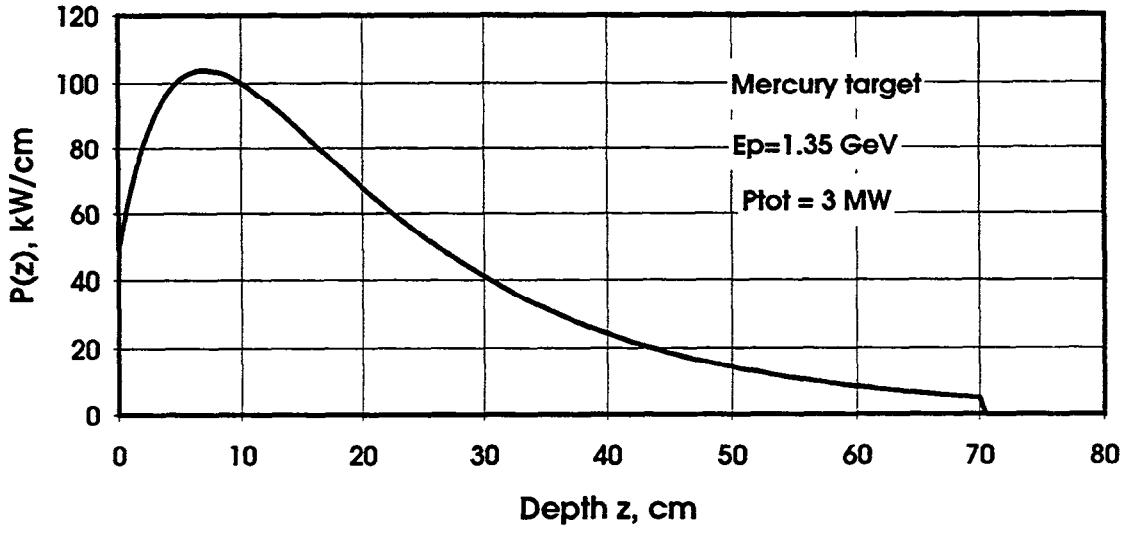

Figure 6: Axial dependence of the power deposition (integral over the beam diameter) used as input for the heating calculations.

The aspect ratio and area of the ellipse representing the target cross section can be varied to examine the effect of travelling times of the pressure waves from their origin to the walls.

Immediate effects are, of course, obtained at the target head where heating occurs directly behind the walls. For all other positions along the container wall the stresses are rather complicated functions of position and time due to the osciallatory behaviour of the system.

In Fig. 7 we show the stress as a function of time obtained for an elliptic target cross section with an area of 707 cm^2 and with an aspect ratio of 3:2 at the points A and B (plane of maximum stress) for the situation of the target with a rigid cover. Clearly one can see the effects of travelling time and of local curvature of the wall:

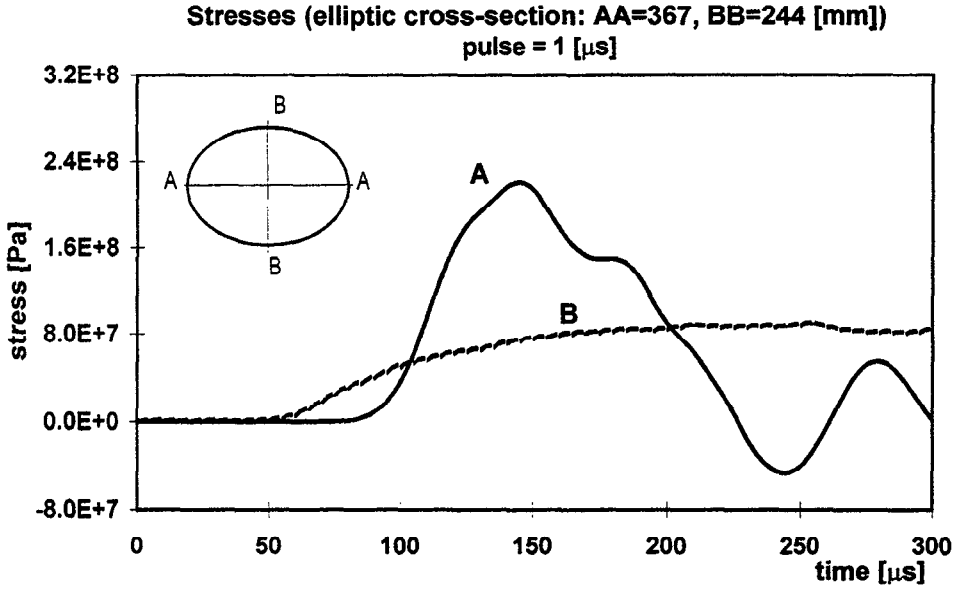

Figure 7: Calculated stress as a function of time for the two positions A and B at the level of maximum stress along the cylinder walls of 8 mm thickness for a 1 μs long power pulse of 60 kJ total engery.

While the pressure wave reaches point B (b=122 mm) about 50 μs after the pulse, the pressure rise is rather moderate due to the softness of the wall at this position (large radius of curvature). The farer point A is reached after 80 μs but the stresses rises much more rapid due to the stronger curvature of the wall at this position. The maximum stress is reached after about 150 μs at a level of 145 MPa. Some oscillatory behaviour is clearly seen in both cases. The maximum level reached is close to the recommended design stress for HT-9-type steels (Fig. 8). Also, it must be noted that this is only the dynamic contribution from the pressure waves in the target and a wall of 8 mm thickness was assumed. This is probably too thick to be cooled. Hence a reduction of the pressure wave contribution is highly desireable.

As an illustrative example we show in Fig. 9 the same geometry but for the case of a 250 μs long proton pulse of the same total energy content. While the curves are topologically similar to those of Fig. 7, the stress level reached is only 10% of the former, mainly dominated by the height of the rising edge of the pulse. This shows that for a long pulse neutron source stress waves in the target should not be a problem.

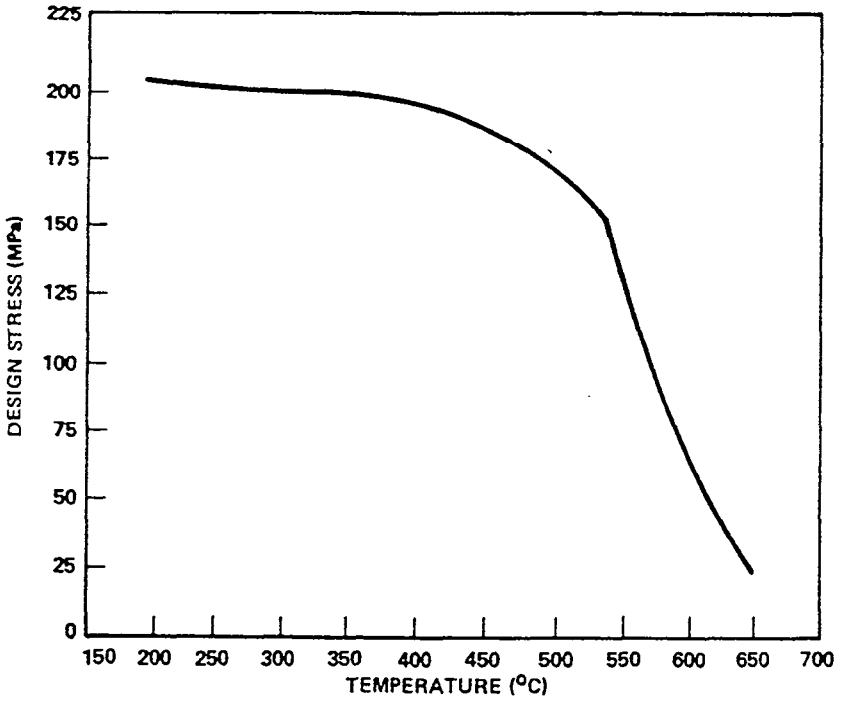

Figure 8: Allowable design stress in HT-9-type steel as a function of temperature (after [5]).

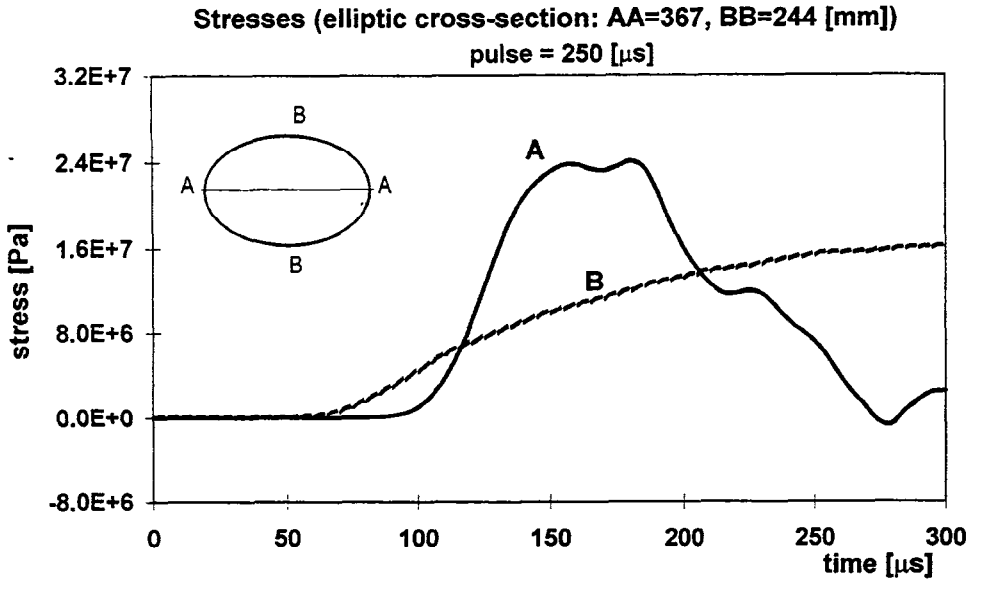

Figure 9: Calculated stress as a function of time for the same situation as Fig. 8, but with an assumed pulse duration of 250 μs.

For the case of a circular target cross section, somewhat higher maximum stress levels are obtained but the difference is not large. Similarly, allowing a free surface or using a domed cover at the point of beam entry has a noticeable but not really significant effect on the maximum stress along the wall.

For the case of the open surface, liquid is found to be expelled through the surface Figs. 10a and b give the velocity profile and the surface contour of the liquid at 300 μs after the beam

hits the target. The maximum velocity obtained can be seen to be of the order of 10 m/s. The profile ressembles very closely to that observed for underwater explosions!

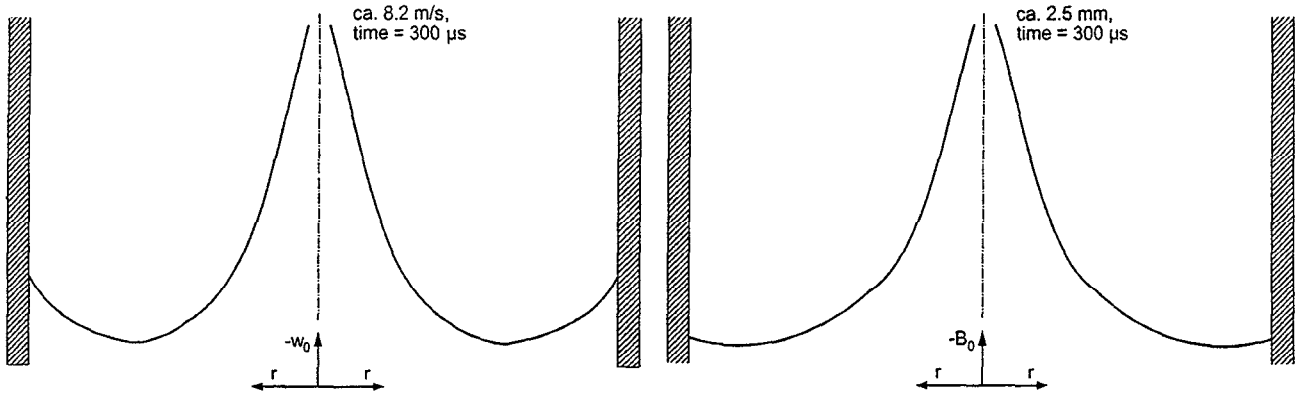

Figure 10: Calculated expulsion of the liquid through the open surface of beam entry for a 1 µs pulse of 60 kJ. (a) Velocity profile at 300 µs after the pulse (b) Surface contour at 300 µs after the pulse.

For the case of an elastic dome-shaped cover the stress distribution along a line running from the apex of the cover down the dome and along the cylindrical wall is shown in Fig. 11 for two different times after the pulse. It can be seen that there results a rather complicated vibrational behaviour which is caused by the elastic properties of the system on the one hand and the different travel times of the pressure waves to the various points along this line on the other. The geometry used here was a cylindrical cross section and a wall thickness reduced to 6 cm which explaines the somewhat higher peak at 150 µs compared to Fig. 8.

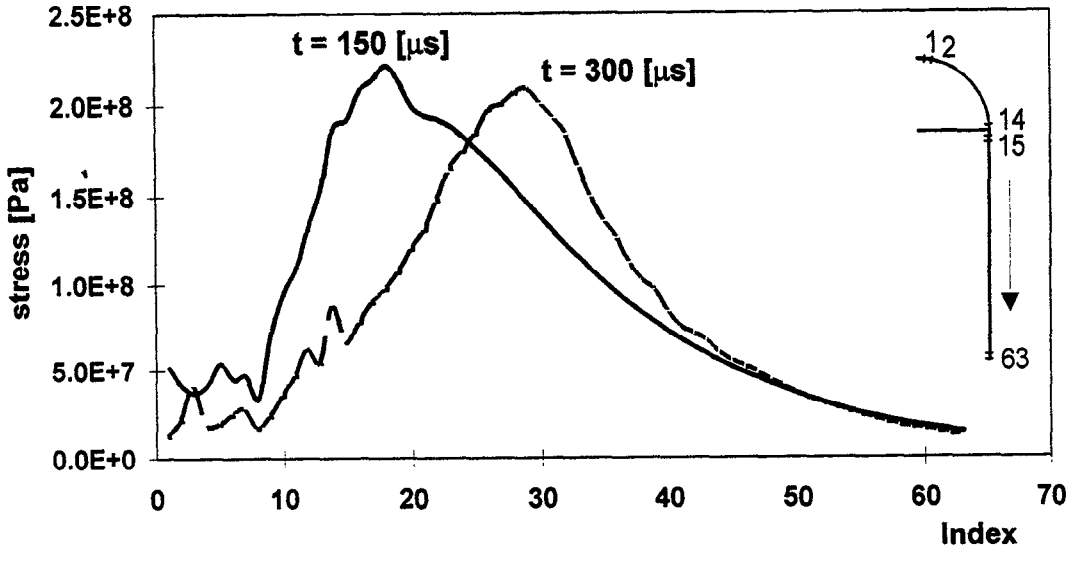

Figure 11: Calculated stress distribution along a line running from the apex of the dome-shaped beam entry window along the dome and down the cylindrical wall (6 mm thick), shown for two different times after the pulse.

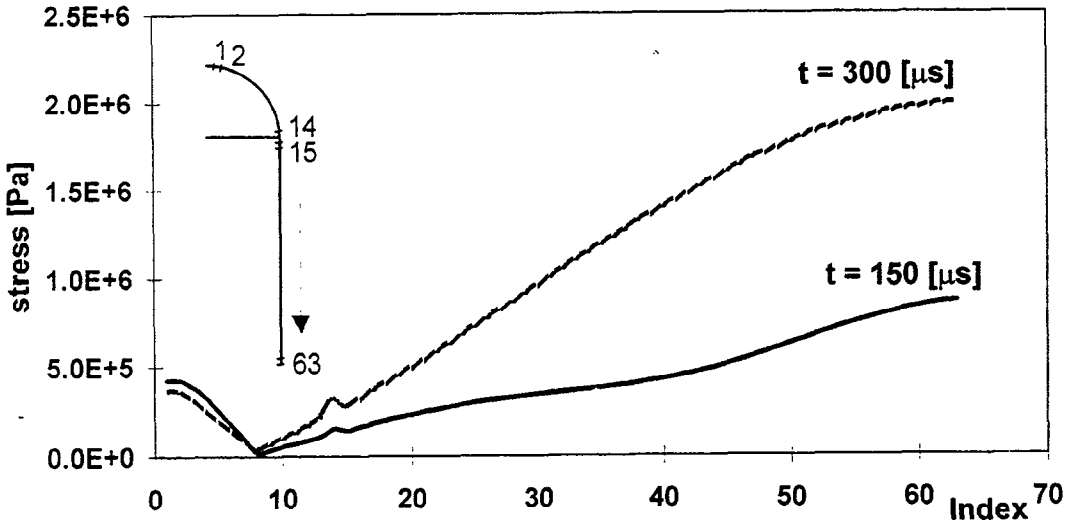

Figure 12: Calculated stress distribution for the same situation as Fig. 11, but with a volume concentration of 3% He in the liquid.

The most significant effect is found after adding a small volume fraction of bubbles to the liquid. Fig. 12 shows the same situation as Fig. 11, but this time 3% of the volume were assumed to be gas bubbles. The maximum stress on the wall has decreased by two orders of magnitude, to an almost insignificant level. It is also obvious that the system reacts much softer with the stress rising during a much longer time after the pulse. As discussed before, this effect depends rather critically on a minimum fraction of bubbles. In the regime where the volume of the bubbles is not enough to accommodate the full expansion of the liquid we find some puzzling effects which we still need to investigate in more detail.

7. Conclusions

While our results are still of preliminary nature in particular as far as absolute numbers are concerned, the program system we have developed clearly allows us to judge the effect of parameter variations such as the pulse duration and the beam geometry in the system. In particular the opportunity of injecting gas bubbles in the beam interaction region might, if a technical solution can be found, provide a means to supress nearly totally the effect of pressure waves. This will make the heat deposition in the window itself, which has so far been neglected completely in our calculations, the main source of stress. From our results we are confident that a liquid metal should be a viable solution not only for continuous sources but also for pulsed sources in the beam power regime of several MW.

8. Acknowledgement

This work has profited from many discussions with various collegues, in particular B. Smith and Y. Takeda. We would also like to thank L. Ni for help with the calculations and producing the figures. The work was carried out in the frame of a grant obtained from the Bundesamt für Bildung und Wissenschaft (BBW-contract Nr. 94.0134) in the context of the Human Capital and Mobility Program of the EU, contract Nr. CHRX-CT94-0503.

9. References

[1] G.A. Bartholomew and P.R. Tunnicliffe (eds.) "The AECL-Study for an Intense Neutron Generator", *Rep. AECL-2600.* (1966)

[2] G.S. Bauer, "SINQ-Status Report Oct. 1990" in *Proc. ICANS-XI,* Tsukuba, KEK-report 90-25 (1991) p. 41-60

[3] G.S. Bauer, H. Sebening, J.-E. Vetter and H. Willax (eds.) "Realisierungsstudie zur Spallations-Neutronenquelle" *Report Jül-Spez-113* and *KfK 3175* Kernforschungsanlage Jülich und Kernforschungszentrum Karlsruhe (1981)

[4] H. Lengeler and J.L. Finney "The European Spallation source", *Europhysics News,* 25, (1994) p.37 - 38

[5] J.D. Gordon, J.K. Garner, N.M. Ghoniem, J. F. Farmer "Ferritic Steel Applications in the MARS High Temperature Blanket" *Proc. Topical Conference on Ferritic Alloys for Use in Nuclear Energy Technologies*, Met. Soc. AIME (1984) pp. 157 - 167

Appendix

A1 Computing the pressure in the liquid metal

General

The pressure being a function of volume V and temperatur T, we have for any differential change:

$$dp = \left(\frac{\partial p}{\partial V}\right)_T dV + \left(\frac{\partial p}{\partial T}\right)_V dT \tag{A1.1}$$

The modulus of isothermal volume compressibility K is defined as

$$K = \left(\frac{\partial p}{\frac{\partial V}{V_0}}\right)_T = V_0 \cdot \left(\frac{\partial p}{\partial V}\right)_T \tag{A1.2}$$

and the coefficient of volume expansion α_v is

$$\alpha_V = \left(\frac{\frac{\partial V}{V_0}}{\partial T}\right)_p = \frac{1}{V_0} \cdot \left(\frac{\partial V}{\partial T}\right)_p \tag{A1.3}$$

If the interval of heating of the liquid volume is very short, the material will not be able to accomodate the resulting change in volume, i.e. we are dealing with the case of isochoric heating (heating at constant volume). After the pulse there is no further heat input and since thermal conduction effects are much slower that the velocity of sound we may safely assume an adiabatic expansion.

Isochoric case:

The change in temperature due to the depostition of an energy ΔQ into a volume element of mass m is

$$\Delta T = \frac{\Delta Q}{m \cdot c_v} \tag{A1.4}$$

with c_v being the specific heat capacity at constant volumes (J/kg K).

Using dV = 0 in eqn. (A1.1) and eqns. (A1.2) and (A1.3) we have

$$\Delta p = \left(\frac{\partial p}{\partial T}\right)_V \cdot \Delta T = \left(\frac{\partial p}{\partial V}\right)_T \cdot \left(\frac{\partial V}{\partial T}\right)_p \cdot \Delta T = K \cdot \alpha_v \cdot \frac{\Delta Q}{m \cdot c_v} \tag{A1.5}$$

Adiabatic case:

Although, in the adiabatic case, the change in pressure is mainly dominated by the first term on the right hand side of eqn. (A1.1), the minor change in temperature is accounted for in our calculations in order to remain as general as possible.

We rewrite eqn. A1.1:

$$dp = \left(\frac{\partial p}{\frac{\partial V}{V_0}}\right)_T \frac{dV}{V_0} + \left(\frac{\partial p}{\partial T}\right)_V dT \qquad \text{(A1.1a)}$$

Using the condition for adiabatic expansion (dQ=0) we have

$$dQ = dU + pdV = Cv \cdot dT + pdV = 0 \qquad \text{(A1.6)}$$

$$\text{with } C_V = m \cdot c_V = \left(\frac{\partial U}{\partial T}\right)_V \qquad \text{(A1.7)}$$

$$\text{or } p = -C_V \cdot \frac{dT}{dV} \qquad \text{(A1.6a)}$$

Using

$$C_p = C_V + p \cdot \left(\frac{\partial V}{\partial T}\right)_p \qquad \text{(A1.8)}$$

and inserting (A1.6a) we obtain

$$C_p - C_V = -C_V \cdot \frac{dT}{dV} \cdot \left(\frac{\partial V}{\partial T}\right)_p$$

which we can rewrite as

$$dT = \frac{\frac{c_p}{c_V} - 1}{\left(\frac{\frac{\partial V}{V_0}}{\partial T}\right)_p} \cdot \frac{dV}{V_0} = \frac{\frac{c_p}{c_V} - 1}{\alpha_V} \cdot \frac{dV}{V_0} \qquad \text{(A1.9)}$$

Inserting (A1.9) into (A1.1a) and using (A1.2) we obtain

$$dp = K \cdot \frac{dV}{V_0} - \frac{\frac{c_p}{c_V} - 1}{\alpha_v} \cdot \left(\frac{\partial p}{\partial T}\right)_V \cdot \frac{dV}{V_0} = K\left(1 - \frac{\frac{c_p}{c_V} - 1}{K \cdot \alpha_v} \cdot \frac{\partial p}{\partial T}\right)_V \cdot \frac{dV}{V_0} \qquad \text{(A1.10)}$$

which, with the help of eqns. (A1.2) and (A1.3) can be rewritten to yield

$$dp = K \cdot \frac{c_p}{c_V} \cdot \frac{dV}{V_0} \qquad \text{(A1.10a)}$$

$$\text{or, } \Delta p = K \cdot \frac{c_p}{c_V} \cdot \frac{\Delta V}{V_0} = \tilde{K} \cdot \frac{\Delta V}{V_0} \qquad \text{(A1.10b)}$$

The quantity $\tilde{K}$ is called the adiabatic modulus of volume elasticity. Its use makes (A1.10b) formally equal to the first term of (A1.1a) but including the effect of the second term. c_v can be calculated from c_p, which is usually known, by using eqns. (A1.8) and eqn. (A1.3):

$$c_p = c_V + p \cdot \frac{\alpha_V}{\rho}$$

with ρ being the density of the material.

ΔV in eqn. (A1.10b) is obtained as a result of all mass displacements into and out of the grid volume considered and is treated as a "virtual" expansion because it is used to compute the resulting change in pressure.

General case of "slow" heating

In order to be able to treat also the more general case, where some expansion can take place during the power deposition period ("long pulse source") we finally consider the non-isochoric case.

Describing the process as a combination of isochoric heating and subsequent adiabatic compression, we can use

$$dT = \left(\frac{\partial T}{\partial V}\right) dV = \left(\frac{\partial T}{\frac{\partial V}{V_0}}\right) \cdot \frac{dV}{V_0} \qquad \text{(A1.11)}$$

and eqn. (A1.3) to justify the relation

$$dT = \frac{1}{\alpha_V} \cdot \frac{dV}{V_0} \quad \text{or} \quad \Delta T = \frac{1}{\alpha_V} \cdot \frac{\Delta V}{V_0} \qquad \text{(A1.12)}$$

which, together with $\Delta Q = C_v \Delta T + p\Delta V$ (eqn. A1.6) yields, for the thermal contribution to the change in volume:

$$\Delta V_{th} = \frac{\Delta Q}{\frac{c_V}{\alpha_V} \cdot \rho + p} \qquad \text{(A1.13)}$$

The first term in the denominator is of the order od 10^{10} N/m^2 for the case of liquid metals and hence at least 1000 times greater than any value of p to be considered. Neglecting p and using eqn. (A1.3), eqn. (A1.13) can be transformed to yield eqn. (A1.4), which shows that the general case is physically not much different from the isochoric case but the amount of energy is deposited over much longer time periods which, at any point in time, makes ΔQ and the resulting pressure much smaller.

A2 The modulus of volume elasticity for a liquid gas-mixture

Assuming we have a mixture of a liquid matrix of volume V_l with finely distributed gas bubbles of volume V_g we write:

$$V_m = V_l + V_g \qquad \text{(A2.1a)}, \qquad dV_m = dV_l \cdot dV_g \qquad \text{(A2.1b)}$$

From the definition V of the modulus of volume elasticity K for the liquid we have

$$dV_l = -\frac{V_{l,0}}{K} \cdot dp \qquad \text{(A2.2)}$$

In order to determine the second term on the right hand side of eqn. (A2.1b) one needs to know whether the compression of the gas is adiabatic (due to the short time involved) or isothermal (due to the fact that the bubbles are very small and their surface is large). The general formula

$$p \cdot V_g^n = p_0 \cdot V_{g,0}^n \qquad \text{(A2.3)}$$

holds for the general case of a polytropic compression with

$$1 \leq n \leq \kappa \qquad \text{(A2.4)}$$

($n = 1$ for purely isothermal and $n = \kappa$ for purely adiabatic compression).

From (A2.3) we have

$$V_g = p_0^{1/n} \cdot V_{g,0} \cdot p^{-1/n} \qquad \text{(A2.5)}$$

and

$$dV_g = -\frac{1}{n} \cdot p_0^{1/n} \cdot V_{g,0} \cdot p^{-(n+1)/n} dp \qquad \text{(A2.6)}$$

Inserting (A2.2) and A2.6) into (A2.1b) we obtain

$$dV_m = -V_{l,0}\left[\frac{1}{K} + \frac{1}{n} \cdot p_0^{1/n} \cdot \frac{V_{g,0}}{V_{l,0}} \cdot p^{-(n+1)/n}\right] dp \qquad \text{(A2.7)}$$

which we formally rewrite as

$dV_m = -V_{l,0} \cdot \frac{1}{K_m} dp$ in analogy to (A2.2). Defining the volume ratio

$$\varepsilon = \frac{V_{g,0}}{V_{m,0}} = \frac{V_{g,0}}{V_{l,0} + V_{g,0}} \qquad \text{(A2.8)}$$

and taking into account that we are only interested in cases where $V_{g,0} << V_{l,0}$ (up to a few percent), we can set

$$K_m = \left(\frac{1}{K_l} + \frac{1}{n} \cdot p_0^{1/n} \cdot \varepsilon \cdot p^{-(n+1)/n} \right)^{-1} \qquad \text{(A2.9)}$$

The magnitude of K_e is of the order of 10^{10} N/m^2 and hence K_m is stronlgy affected by ε. Since we don't know exactly what value of n to use, we remain on the safe side (less reduction of K_m relative to K_l, if we use the case of isothermal compression (n=1), although for very short pulses adiabatic compression of the gas bubbles seems more likely.

For He-gas we have $\kappa = 1.63$ and hence

$$1 \leq n \leq 1.63 \qquad \text{(A2.10a)}$$

$$2 \geq n+1/n \geq 1.61 \qquad \text{(A2.10b)}$$